Mitochondrial Function and Optical Properties of the Crystalline Lens

by

Kenneth Wayne Olsen

A thesis
presented to the University of Waterloo
in fulfilment of the
thesis requirement for the degree of
Master of Science
in
Vision Science and Biology

Waterloo, Ontario, Canada, 2008

AUTHOR'S DECLARATION

I hereby declare that I am the sole author of this thesis. This is a true copy of the thesis, including any required final revisions, as accepted by my examiners.

I understand that my thesis may be made electronically available to the public.

ABSTRACT

The crystalline lens is a unique cellular organ that performs metabolic processes while maintaining optical functionality. Mitochondria play a vital role in providing the cell with the energy necessary for these metabolic processes and have recently been shown to be more metabolically active than previously thought.

To test the hypothesis that mitochondrial function directly influences the optical function of the lens, bovine lenses were treated with 50 μM, 200 μM, 600 μM and 1000 μM menadione, a mitochondrial specific toxin that renders the mitochondria inactive, and the Back Vertex Distance (BVD) variability was observed over 216 hours. Confocal micrographs of secondary fibre cells' mitochondria were also analyzed for 50 μM, 200 μM, and 600 μM menadione treatment over 48 hours. Increase in BVD variability (± s.e.m.) was observed within 24 hours from 0.28 ± 0.021 to 1.83 ± 0.75 for the 600 μM treated lenses. Confocal micrograph analysis showed a trend toward a decrease in the average length of mitochondria from 7.9 ± 0.8 to 3.7 ± 0.9 over for 200 μM treated lenses and from 5.9 ± 1.0 to 3.6 ± 0.6 for the 600 μM treated lenses over 48 hours.

These data show that indeed menadione has a detrimental effect on mitochondria as a function of both time and concentration and this change in mitochondria precedes changes in BVD variability directly linking mitochondrial function to optical function.

ACKNOWLEDGEMENTS

I would like to thank my supervisor Dr. Vivan Choh for her time, patience, and guidance throughout my graduate studies and for always encouraging me to do a little more, push a little harder and look a little deeper. I also thank Dr. Vladimir Bantseev who started me on this path and for his wisdom and experience that he freely shared with me. I am grateful to my committee members Drs. Jake Sivak and George Dixon for their invaluable insight and direction throughout my project.

A big thanks goes to all those who assisted me in my research from going on eyeball pick-up runs to cleaning up after me. Many thanks to my colleagues who listened to me when I had question and discussed ideas on how to overcome obstacles with me. Without the wonderful services of Cargill Meat Solutions (formerly Better Beef) this research would not have been possible, and a special thanks goes to all the hundreds of cows who sacrifice made this research possible.

My family and friends played a large part in the completion of this thesis by lending a hand in whatever way they could, including many meals and tanks of gas. Most of all, I want to thank my wife for her support and sacrifice during late nights and long experiments and for always believing in me. I could not have done this project without her.

DEDICATION

This thesis is dedicated to my wonderful daughter

Talia Mae.

Your encouragement:

"Are you going to school? So you can learn? Okay, you go to school"

and endless love:

"I want to sing, 'I'm So Glad When Daddy Comes Home?'"

gave me strength, motivation, and joy.

I love you!

Table of Contents

List of Tables

List of Figures

1. Introduction

As a living and constantly growing tissue the crystalline lens must carry out the usual metabolic processes required for maintenance and growth, for which ATP is essential, while also ensuring transparency to allow for the proper optical functionality of fine focusing light onto the fovea of the retina. While originally thought to be absent from fibre cells of crystalline lenses, and few in number within lens epithelial cells, mitochondria have recently been shown to be more numerous (Bantseev et al., 2003a) and more dynamically active (Bantseev and Sivak, 2005) in both cell types than was previously thought. These new findings suggest that mitochondria contribute more to overall lens metabolism than was once believed.

Since mitochondria are large enough to scatter light (Benedek, 1971), a natural part of lens cellular differentiation includes the degradation and disappearance of all membrane bound organelles (including mitochondria) that lie in the path of light (Bassnett and Mataic, 1997). Disruption of this natural process, including the premature inactivation of the mitochondrial oxidative phosphorylation, caused by toxins such as carbonyl cyanide m-chlorophenylhydrazone, causes opacities, known as cataracts, to form in the lens (Bantseev et al., 2003b; Bantseev et al., 1999). This suggests that while they occupy only a minute portion of the cell and only in the cells of the superficial

fibres, mitochondria play a great role in lens metabolism and possibly cataract formation.

The purpose of this study is to investigate the relationship between mitochondrial function and optical function of the crystalline lens using the mitochondrial uncoupler menadione. As no studies to date have been performed on cultured bovine lenses using menadione, the effectiveness of menadione as a mitochondrial uncoupler must also be verified.

2. Literature Review

2.1. The Crystalline Lens

2.1.1. Human Crystalline Lens Development

The crystalline lens begins to form during embryonic development with the formation of the lens placode. The lens placode is formed by the thickening of surface ectodermal cells through induction by the optic vesicle which they surround (O'Rahilly and Meyer, 1959). Following ectodermal cell induction the optic vesicle begins to fold inward to form the optic cup. At the same time that the optic cup is forming, the cells of the lens placode begin to invaginate on themselves. The final step of the invagination process is the complete detachment of the lens placode from the surrounding tissues forming a hollow sphere called the lens vesicle (Kuszak et al., 1980). The cells of the lens vesicle have essentially turned "inside-out" with the basal end of the cells on the outside of the tissue. This orientation is one reason for the crystalline lens' unique growth and development, as well as its distinctive somatic features. At the location on the lens placode, where it detached itself from the surface ectoderm, the lens capsule begins to form and will be the future structure to which the suspensory ligaments, known as the zonules of Zinn, will attach (Seland, 1992).

Induction of the cells found in the posterior portion of the lens vesicle by the retina causes these cells to differentiate, resulting in the elongation of the previously cuboidal cells into very long and thin cells filling the hollow space of

the lens vesicle (Kuszak et al., 1985). These are the first cells of the lens to differentiate into fibre cells and are referred to as the primary fibre cells and the nucleus of the lens. It is due to this induction that no epithelial cells are found on the posterior side of the crystalline lens. Those cells that remain on the anterior surface of the lens vesicle will eventually form the lens epithelial cells.

2.1.2. Lens Growth

Epithelial cells located within the peripheral zone of the lens, just anterior to the equatorial zone, in the region known as the germinative zone, undergo mitosis and are responsible for the growth of the lens. As these cells divide, they migrate toward the equatorial zone and differentiate into secondary fibre cells (Harding et al., 1971).

The crystalline lens continues to grow in this manner with epithelial cells migrating to the equator and differentiating throughout life. Because the lens cells are inverted, with the basal side facing out, the secondary lens fibre cells continue to condense and compact on top of each other as the lens grows. This causes the diameter of the lens to increase throughout life, though due to the compactness of the fibre cells, the increase is small. Because the cells are compacting onto each other, a gradient of densities is created with the nucleus being the densest with a refractive index of approximately 1.41, and the periphery being the least dense with a refractive index of approximately 1.37 in humans (Kasthurirangan et al., 2008; Trokel, 1962). The gradient index is critical for preventing longitudinal

spherical aberrations, the loss of sharp focus due to the light rays exiting an object with a spherical surface at the periphery having a different focal point than those passing through the centre. The difference in refractive indices allow for fine focusing of images on the retina and have recently been shown to adjust throughout life (Augusteyn et al., 2008; Mcavoy, 1978).

2.1.3. Secondary Fibre Cell Differentiation

In addition to providing continual growth for the lens, lens fibre cell differentiation also plays a vital role in maintaining transparency of the lens. Organelles such as the nucleus, golgi apparatus, endoplasmic reticulum, and mitochondria are potential light scattering objects due to their size and high index of refraction (1.39-1.6) compared to their surrounding cytoplasm environment (approximately 1.37) (Amos and Klug, 1974; Beauvoit et al., 1994; Brunsting and Mullaney, 1974; Wilson and Foster, 2007; Wilson et al., 2007). During the process of fibre cell differentiation, not only do the cells elongate, stretching between the epithelial cells and the existing fibre cells at the anterior pole to the posterior pole of the lens, but organelle degradation is also observed to occur, preventing light scatter (Bassnett, 1995; Bassnett and Beebe, 1992; Bassnett and Mataic, 1997; Dahm et al., 1998). The area of the lens where no more organelles are found is known as the organelle free zone (OFZ).

Secondary fibre cells that still contain their organelles are only found to be within the shadow of the iris close to the periphery of the lens penetrating

approximately 15% of the total width of the lens, while the OFZ is found along the pathway of light through the lens (Bassnett, 2002; Bassnett and Beebe, 1992). Because of this, light scatter is minimized allowing for clear images to be formed on the retina.

Organelle degradation begins with the changing of the nuclear shape from ovoid to spherical followed by a dismantling of the nuclear lamina and finally disintegration of the chromatin (Bassnett and Mataic, 1997; Dahm et al., 1998). Unlike other animals, complete DNA disintegration in humans is much slower, with small DNA particles persisting in the cytoplasm for weeks or months (Bassnett, 1997). Once the DNA begins to breakdown, a rapid loss in all other organelles is seen to follow, a process completed within a few cell layers which represents as little as 2-4 hours (Bassnett and Beebe, 1992). However, this order of organelle degradation does not appear to be a result of DNA breakdown nor occur in a sequential order, but rather relies on independent pathways as organelles are seen to disappear even when denucleation is inhibited (Nishimoto et al., 2003).

2.1.4. Crystalline Lens Metabolism

The fully developed lens is a self contained organ that is suspended in the eye and located immediately behind the retina by fibres known as zonules of Zinn. These zonules attach from the ciliary process and valleys to the lens capsule and, in humans, assist in accommodation by dynamically changing of the shape of the

lens to allow for the focusing of nearby object (Bornfeld et al., 1974). Due to the lens being suspended by these fibres and in order to prevent light scatter, the lens contains no vasculature on which to rely for nutrients or disposal of waste. As such, the lens relies on an internal micro-circulatory system to create a flow of fluids (Mathias, 1985; Mathias and Rae, 1985; Robinson and Patterson, 1983). Fluids enter the lens through the centre of both the anterior and posterior poles, through the lens toward the nucleus, and then flow out of the lens through the equatorial region. The driving force of this current is believed to be due to the flow of sodium (Na^+).

High concentrations of Na/K ATPase pumps are found in the equatorial zone of the epithelial cells of the lens, which maintains a low intracellular Na^+ concentration and a high intracellular K^+ concentration (Mathias et al., 1997; Paterson, 1972; Paterson et al., 1974). The ATPase pumps generate a concentration gradient of Na^+ with a higher concentration found toward the centre of the lens than is found at the equator. This gradient draws the Na^+ toward the epithelial cells, first from then center of the lens and then the poles, as they flow from areas of high concentration to those of low concentration, by passing through the many gap junctions that connect the fibre cells as well as between the cells (Benedetti et al., 1976). This flow of Na^+ creates a net circulatory current of ions, water and nutrients that enters the anterior and posterior poles and exits the

equatorial region creating a complete cycle which ensures a constant replenishment of nutrients and waste removal from the lens.

Though not a significant contributing factor to the current flow within the lens, the role of K^+, or perhaps rather lack thereof, is worthy of note. Fibre cells appear to have a low conductance for K^+, meaning that it does not passively flow from the area of high concentration within the epithelial cells into the fibre cells, and simply leaks back out the same epithelial cells that pumped them in (Candia and Zamudio, 2002; Mathias and Rae, 1985). If K^+ were able to flow into the fibre cells, the opposite direction from the Na^+ flow, it would counter the effects of the Na^+ and reduce or inhibit the net circulation. Therefore, it is very important that fibre cells remain resistant to the influx of K^+.

2.1.5. Lens Cataract Formation

As long as the lens develops, continues to grow with normal fibre cell differentiation, and can maintain its metabolism, it should remain clear and cause no problems in vision. Should any of the normal processes go awry, however, opacities can be seen in the lens, causing a scattering of the light, and result in a decrease of visual acuity or, should the opacity be severe enough, blindness. These opacities are collectively known as cataracts for which there are several types, including nuclear, cortical, posterior subcapsular, galactose, Nakano, and radiation cataracts. Each of these is associated with its own set of risk factors like diabetes, alcohol, or medications as well as its own mechanism through which the

opacities form, such as crystalline aggregation or reduction, pyruvate accumulation, or cytoskeletal disorientation (Azuma et al., 2003; Dische et al., 1956; Dische et al., 1959; Fukui et al., 1976; McCarty and Taylor, 1996).

Despite the many types of cataracts and seemingly endless list of risk factors and triggers, there appear to be three main underlying mechanisms through which cataract formation occurs: oxidative stress, blockage of lens micro-circulation, and degradation of microfilaments (Eckert et al., 2000; Shearer et al., 1997; Williams, 2006).

Oxidative stress may be most common mechanism for cataract formation as this stress can be caused by a variety of factors including UV exposure, diet, diabetes, and dehydration (Taylor, 1999). Oxidative stress inside the cell leads to a formation of the superoxide radical which reacts with the thiol groups of crystalline protein and generates disulfide bridges to form between crystalline proteins causing protein aggregates to form which scatters light and therein a cataract (Ozaki et al., 1987).

A second mechanism of cataract formation involves the interruption of the lens micro-circulation. Gap junctions found in the fibre cells of the lens, vital to maintaining the circulation, have been shown to be sensitive to pH (Bassnett and Duncan, 1988). Due to the lack of mitochondria near the centre of the lens, lactate, a product of glycolysis, can accumulate which causes the pH to drop. Under normal conditions, the circulation within the lens is sufficient to prevent an

accumulation of lactate. However, some conditions, such as increase uptake of glucose, can increase the acidity to a pH of 6.5 (Bassnett and Duncan, 1988; Mathias et al., 1981). This low pH causes the gap junctions to close and swelling of the cells is observed resulting in a disorganization of the proteins, causing light to scatter and the cataract to form.

The final mechanism that will be discussed is in relation to the cytoskeleton of the lens. This mechanism is dependent on an increase in cytoplasmic calcium which activates the protease calpain found within the cells. Once activated, this protease begins to cleave the microfilament proteins (actin and microtubules) as well as the crystallins (Azuma et al., 1995; Sanderson et al., 1996). This breakdown of the cytoskeleton begins the process known as globulization, the breaking apart of the cell into multiple small round cells, which are light scattering (Bhatnagar et al., 1995).

2.2. Mitochondria

2.2.1. Mitochondrial Structure

Mitochondria, whose name was coined from the Greek words mitos meaning tread and khondrion meaning granule, have been observed since the nineteenth century and were named by Carl Benda, a German microbiologist, in 1898. It was originally hypothesized in 1923 that mitochondria were once a distinct aerobic bacteria that were introduced into anaerobic eukaryotes through endocytosis (Wallin, 1923). This endosymbiotic hypothesis, however, was given

little attention until Lynn Margulis' publication of *Symbiosis in Cell Evolution* in 1981, when the idea became widely accepted. While this theory is still the most commonly accepted, there are others that exist. One theory that has been growing in popularity, due to findings in DNA fingerprinting, suggests that rather than a eukaryote engulfing a prokaryote to form some sort of super-eukaryote, two individual bacteria, one aerobe and one anaerobe, were fused together to form a primitive eukaryote, containing mitochondria, from which all present eukaryotes evolved (Gray et al., 1999; Vellai and Vida, 1999).

Although mitochondria had been seen and studied for many years, observations of the internal structure of the organelle were not made until the early 1950's with the help of the electron microscope. Primary observations showed that mitochondria were composed of two bi-lipid membranes: an exterior membrane, separating it from the cytoplasm, as well as an interior membrane that surrounds a matrix (Palade, 1952). The interior membrane was seen to form "internal ridges" which were given the name "cristae mitochondriales". These ridges were thought to be shelf like protrusions toward the centre of the mitochondrion along the short axis at regular intervals which nearly reached to the opposite side. The cristae described by Palade are said to be "baffle-like" (similar in shape to a radiator) and it is this idea of the internal structure that has dominated since. These protrusions of inner membrane into the matrix increase the surface area of the membrane maximizing ATP synthesis through oxidative

phosphorylation. While the idea of a convoluted inner membrane still exist today, recent observations using improved techniques and technology are disputing the simple "baffle-like" organization for a much more complex and irregular inner membrane organization, including the formation of tunnel-like structures that extend all the way through from one side of the matrix to the other (Mannella, 2000; Perkins and Frey, 2000).

2.2.2. Mitochondrial Function: ATP synthesis

Current data show that within the crystalline lens mitochondria account for approximately 33% of all ATP produced while the remaining ATP results from glycolysis (Trayhurn and Van Heyningen, 1972). Mitochondria generate ATP through a process known as oxidative phosphorylation that takes place within and across the inner mitochondrial membrane (see Figure 1). The inner membrane consists of only 27% lipid with a staggering 73% protein composition, the majority of which includes the five protein complexes that are responsible for the generation of ATP from ADP within the mitochondrial matrix (Fleischer et al., 1961). These five protein complexes that make up the oxidative phosphorylation system are:

1) NADH:ubiquinone oxidoreductase (complex I)

2) Succinate: ubiquinone oxidoreductase (complex II)

3) Ubiquinol: ferricytochrome c oxidoreductase (complex III)

4) Ferrocytochrome c: oxygen oxidoreductase (complex IV)

5) ATP synthase (complex V) (Hatefi, 1985).

Ubiquinone, also known as coenzyme Q, and cytochrome c, along with a few other electron carriers, play a vital role within this system of carrying electrons from one protein to the other to generate the energy needed for the process; this flow of electrons through the various proteins is known as the electron transport chain, or respiratory chain (Chow and Biale, 1957).

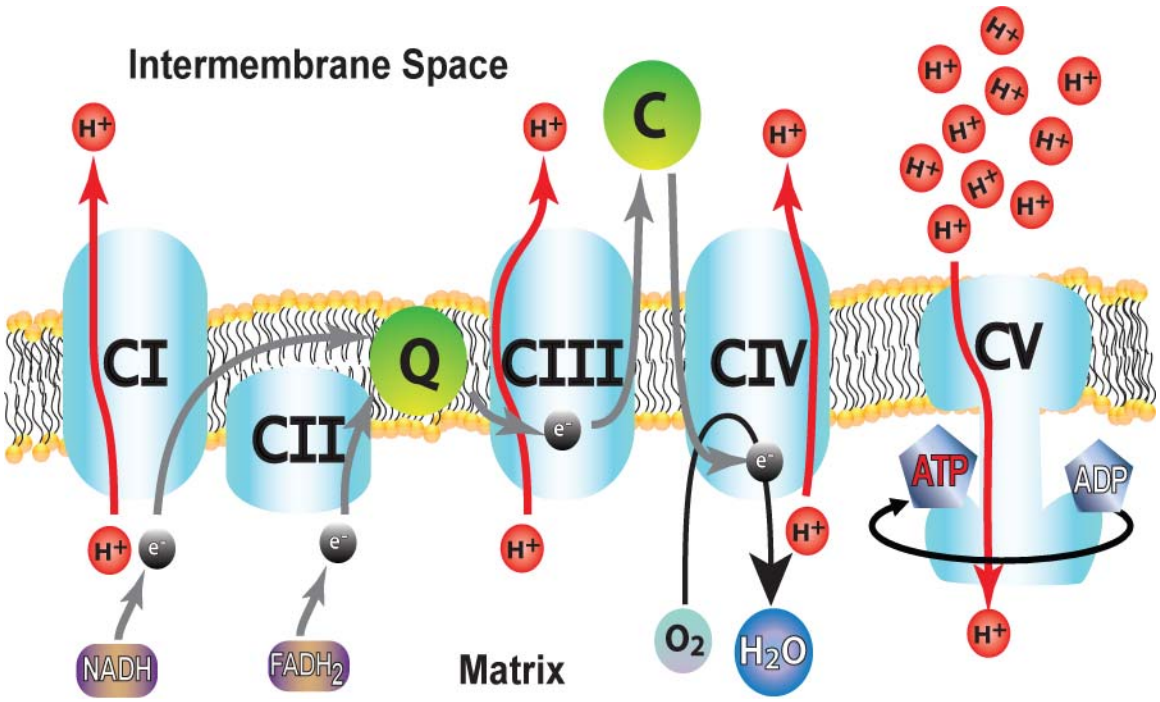

Figure 1: A schematic diagram of oxidative phosphorylation and the electron transport chain. Protein complexes I through V (CI-CV) are shown embedded within the inner membrane of the mitochondria along with the electron carriers ubiquinone (Q) and cytochrome c (C). Electron (e^-) flow is shown by gray arrows and proton (H^+) flow is shown by red arrows. Refer to text for details.

The respiratory chain begins with a redox reaction of an electron (e^-) being transferred from a molecule of NADH to ubiquinone (Q) through complex I generating a ubisemiquinone radical and NAD (Hatefi and Stempel, 1969). The energy released allows for two protons, or hydrogen ions (H^+), to be pumped from the matrix into the intermembrane space creating an electrochemical proton gradient ($\Delta_\psi m$) across the inner membrane. This proton gradient is essential to drive the final step of oxidative phosphorylation. Following a second cycle of NADH being oxidized to NAD, a second electron is transferred to the ubiquinone radical fully reducing this molecule, now known as dihydroubiquinone, and two more protons are again pumped into the intermembrane space for a total of 4 protons. The dihydroubiquinone then carries the electrons to complex III. It is also possible, under the unusual pH condition of ≤ 6, for this complex to oxidize NADPH to NADP, in which case the flow of electrons and the pumping of protons remains the same as per the case of NADH oxidation (Hatefi and Stempel, 1969).

Similarly, complex II transfers electrons from $FADH_2$ to ubiquinone in a redox reaction manner oxidizing the $FADH_2$ to FADH and generating a ubisemiquinone radical after the first electron transfer and dihydroubiquinone after the second (Hatefi and Galante, 1980). In contrast to complex I, however, there is no proton pumping from the matrix to the intermembrane space coupled with this transfer of electrons. The dihydroubiquinone then again carries its newly acquired electrons to complex III.

Ubiquinone, in the form of dihydroubiquinone, is responsible for transferring electrons from complex I and II to complex III, and as it does so, 2 protons are again pumped into the intermembrane space bringing the total thus far to 6 (Leung and Hinkle, 1975). Complex III transfers 2 electrons from ubiquinone to cytochrome c (C) which also results in two more protons being pumped into the intermembrane space (Wikstrom et al., 1981).

Cytochrome c continues along the respiratory chain to complex IV, where the final stage of the respiratory chain occurs. The electrons transferred from cytochrome c to complex IV are used to generate 2 molecules of H_2O from one molecule of O_2 (Babcock and Wikstrom, 1992). For each molecule of H_2O formed, 2 more protons are pumped into the intermembrane space bringing the final count to 10 protons (Gennis, 1998). The generation of H_2O completes the respiratory chain portion of oxidative phosphorylation.

The electrochemical gradient formed by the high concentration of protons within the intermembrane space as compared to the matrix due to the pumping of protons from the mitochondrial matrix to the intermembrane space by complexes I, III, IV and ubiquinone, creates a potential for the protons to re-enter the matrix. They can only do so, however, through the fifth and final protein complex of the oxidative phosphorylation process, ATP synthase. ATP synthase (complex V) had been seen for many years, but it was only in 1997 when the breakthrough discovery was made that not only is this protein an enzyme, but it is in fact a tiny

motor as well which rotates at approximately 100 Hz (Noji et al., 1997). As protons enter the matrix from the intermembrane space, power is provided for the γ subunit of the protein to rotate in a counter clockwise direction (as viewed from the membrane) which drives the generation of ATP from ADP (Itoh et al., 2004; Noji and Yoshida, 2001; Senior and Weber, 2004).

2.3. Mitochondrial Dynamics: Microtubules

2.3.1. Microtubule Structure and Dynamics

Microtubules are polymers of the protein tubulin and are found in most differentiated cells (Burns, 1991; Weisenberg and Taylor, 1968). They play a vital role in the organization of the cytoplasm as well as provide structure and support for the cell. Tubulin is the heterodimer subunit of microtubules and is comprised of a α- and β-tubulin monomers which are approximately 50% identical in their amino acid composition and arrange themselves in a "head-to-tail" fashion: the α-tubulin monomer of one heterodimer always binds to the β-tubulin of the one before (Amos and Klug, 1974). The completed microtubule structure is a hollow cylinder with a diameter approximately 25 nm wide (Desai and Mitchison, 1997).

Since their early discovery, microtubules have been seen to be very dynamic and are now known to exhibit extreme dynamic behaviours. The regular model, referred to as dynamic instability, consists of microtubules rapidly switching from polymerization to depolymerization at the plus end. A second process called treadmilling, initially only observed for in vitro models, consists of

polymerization at one end (either plus or minus) with depolymerization at another (Kirschner and Mitchison, 1986; Margolis and Wilson, 1998).

The mechanism behind polymerization and depolymerization appears to be a cap comprised of a single layer of tubulin GDP-P_i subunits (Panda et al., 2002). When the cap is present on the microtubule end, polymerization can be carried out by adding tubulin dimers using GTP as an energy source. When the cap is removed, rapid disassembly of the microtubule end occurs releasing the tubulin dimers of the filament (Melki et al., 1989). Microtubules have been shown to cause structural changes of cells through pushing forces by polymerization and pulling forces by depolymerization (Inoue and Salmon, 1995).

2.3.2. Microtubule Motors

Microtubules play a primary role in the organization of the cytoplasm and are often considered to be the highways on which various objects (commonly referred to as cargo) transported. The cargo, however, cannot supply the power needed to move along the microtubules and must rely on the motor proteins to carry them around. The first identified family of motor proteins was dynein which showed a unidirectional force on microtubules resulting in a movement toward the minus end (Gibbons, 1981). It wasn't until a few years later when the second family of motor proteins, kinesin, was identified and observed to exert a force on the microtubules in the opposite direction from that of dynein, which showed movement toward the plus end (Vale et al., 1985a; Vale et al., 1985b).

As both dynein and kinesin had shown movement in only one direction, and opposite to each other, it was commonly accepted that cargo travelling toward the plus end of the microtubule was bound to the kinesin motor while cargo moving toward the minus end of the microtubule was bound to dynein. This model of uni-directional movement held for many years until technology improved and it was observed that many cargo, including mitochondria, pigment granules, mRNA particles, vesicles, intermediate filaments and even some pathogens, such as Herpes virus, adenovirus and HIV particles, exhibited a peculiar form of movement in that while the net movement of a cargo is toward one of the microtubule poles, that movement is interrupted by a brief reversal of direction every so often, known as bi-directional movement (de Heredia and Jansen, 2004; Helfand et al., 2003; McDonald et al., 2002; Smith et al., 2001; Suomalainen et al., 1999; Waterman-Storer et al., 1997; Wu and Hammer, 2000).

While it is not clear why this behaviour exists, or even the mechanism behind how this sudden change in direction can occur, and for only a brief moment, it has been shown that there are somewhere around 2 to 5 active motor protein units per cargo at any given time (Ashkin et al., 1990; Gross, 2004; Habermann et al., 2001). These findings have led to a number of models for bi-directional movement including; 1) the "tug-of-war model" where net movement is determined by the relative number of each motor bound to the cargo, 2) the "exclusionary-presence model" where only one type of motor can bind at a time

but does so in a competitive manner, and 3) the "coordination model" where both motors are attached to the cargo simultaneously, but are somehow regulated such that only one is active at any given time (Gross, 2004).

Mitochondria, which are of particular interest to this study, show a tendency to be localized in areas of the cells with a high ATP demand. Cells appear to not rely on diffusion of ATP to the various locations within the cells despite their small size and the ease with which they can and do diffuse. This would be expected as is seen in neuronal axon growth where mitochondria are observed to be concentrated near the growth cone (a long distance away from the cell body), but this is observed even within small cells, such as epithelial cells, this is found to be true (Morris and Hollenbeck, 1993; Vanblerkom, 1991).

In order for mitochondria to travel to areas of high ATP demand, it must do so via microtubules, and indeed have been seen associated with microtubule networks within the lens (Bassnett and Beebe, 1992). Mitochondria have, in fact, recently been shown to be much more dynamically active than was previously thought suggesting a greater role in lens metabolism than was believed (Bantseev and Sivak, 2005). As such, disruption to the normal mitochondrial function would have a great impact on the condition of the lens as a whole as well as on the cellular level.

2.4. Menadione

Menadione (2-methyl-1,4-naphtoquinone), also known as vitamin K_3, is a member of the quinone family consisting of compounds that contain two carbonyl groups and have the general structure O=C—$(C=C)_n$—C=O (Morton, 1965). Though low concentrations of menadione are commonly found in the natural diet of humans, primarily green vegetables, menadione has proved to be toxic at higher levels with the mitochondria being its principle target (De Marchi et al., 2003; Laux and Nel, 2001).

Like other quinones, menadione is an oxidizing agent (electron acceptors) which can undergo either a one- or two-electron reduction. In cells, the main enzyme found to undergo two-electron reduction is the flavoprotein DT-diaphorase which generates a harmless hydroquinone (Thor et al., 1982). NADH:ubiquinone oxidoreductase (complex I of the respiratory chain in mitochondria) is one such enzyme that catalyzes the one-electron reduction which results in damage to the cell (Iyanagi and Yamazaki, 1970). While other enzymes have also been found to catalyze the one-electron reduction, they do not appear to play an important role in the toxic effects of menadione, as those effects can be eliminated by blockage of only complex I (Shneyvays et al., 2005). Therefore, it is complex I that appears to be the main cause for the cytotoxic effects which will be discussed more fully hereafter.

Due to its low molecular weight, menadione easily diffuses into the inner matrix of the mitochondria where it is reduced by complex I of the respiratory chain generating a semiquinone radical (Iyanagi and Yamazaki, 1970). In the presence of molecular oxygen (which is in rich abundance within the mitochondrial matrix), the semiquinone radical enters into a redox cycle with the oxygen resulting in the production of H_2O_2 which is detrimental to the cell as it can react rapidly and non-specifically with most anything it comes in contact with. As the semiquinone radical reacts with the molecular oxygen, menadione is regenerated, free to be reduced yet again by complex I resulting in the redox cycle that is characteristic of radicals. Oxidation of pyridine nucleotides, such as adenosine of ATP, also occurs, which, along with the oxidative stress of the reactive oxygen species, appears to lead to the formation of the membrane permeability transition pore (MPT) (De Marchi et al., 2003).

The MPT is a non-specific, bi-directional pore that allows large objects to freely pass through the inner membrane of the mitochondria, and though its existence is known, the mechanism by which this pore is formed is still not fully understood (Hunter et al., 1976; Zhang and Armstrong, 2007; Zoratti and Szabo, 1995). There are many complications that arise from the formation of the MTP, including efflux of calcium and cytochrome c, as well as the collapse of the electrochemical proton gradient across the inner membrane rendering the mitochondria incapable of generating ATP (De Marchi et al., 2003; Frey and

Mannella, 2000; Haworth and Hunter, 1979; Laux and Nel, 2001; Toninello et al., 2004; Verrax et al., 2006).

While it is agreed that the formation of the MTP contributes in large part to cell death, and indeed may be the trigger for it, the exact factors that are involved, the mechanism used, and even whether cell death occurs by apoptosis or necrosis is still widely debated (Baines et al., 2005; Criddle et al., 2006; Nakagawa et al., 2005; Zhang and Armstrong, 2007).

3. Materials and Methods

3.1. Organ Culture

3.1.1. Eye Dissection

Whole bovine eyes were obtained from a local abattoir (Cargill Meat Solutions Ltd., Guelph, ON). Lenses were carefully excised under sterile conditions and incubated at 37˚C with 5% CO_2 and replaced with fresh culture medium every 48 hours. Following 24 hours of incubation lenses were visually inspected and those showing signs of damage were discarded.

3.1.2. Culture Medium

Bovine lenses were cultured in M199 culture medium (SIGMA, M3769) modified with 26.2 mM sodium bicarbonate, 25.0 mM 4-(2-Hydroxyethyl)piperazine-1-ethanesulfonic acid (HEPES), 0.68 mM L-glutamine, 0.7% sodium hydroxide, 1% penicillin/streptomycin and 3% qualified foetal bovine serum.

3.2. Lens Treatment

Under sterile conditions, the lenses were placed in culture medium containing 0 μM (control, n=10), 50 μM (n=9), 200 μM (n=9), 600 μM (n=8), and 1000 μM (n=9) of menadione for 30 minutes at room temperature. Lenses were then washed three times with 0.9% saline solution, once in serum-free M199 and then returned to their chambers containing fresh M199. Lenses used as control

vehicles (n=10), herein referred to as 0 μM treated lenses, were treated and washed in the same manner but with medium containing no menadione.

3.3. Assessment of Optical Function

Lens optics were assessed using the Scantox™ *In Vitro* Lens Assay System, developed at the University of Waterloo, which measures the back vertex distance (BVD) at various eccentricities from the optical axis. The system consists of a laser that is reflected through the lens under investigation. Two cameras are used to capture the path of the laser. The distance between the most posterior point of the lens (the back vertex of the lens) and the point at which refracted lasers cross the optical axis (focal point) is the BVD. In this study lenses were optically scanned prior to treatment and at 4, 24, 48, 144, and 216 hours post treatment using 22 laser passages per lens per time point. BVD variability, measured as standard error, was used as an indicator of optical quality with greater BVD variability indicating worse optics. Only lenses with pre-treatment BVD variability values between 0.200 and 0.400 mm were included in this study.

3.4. Assessment of Secondary Fibre Cell Mitochondrial Integrity

Following the treatment outlined in section 3.2, lenses were carefully removed from their chambers and placed into Wheaton-33 sample glass vials containing 10 ml serum-free M199 at 37˚C. The lenses were loaded with 20 μM Rhodamine 123 (Molecular Probes, R-302) for 20 minutes at 37˚C and rinsed in

serum-free M199. Rhodamine 123 is a non-cytotoxic, positively charged fluorescent probe that specifically stains active mitochondria as it is attracted to the negatively charged space within the mitochondrion (Johnson et al., 1980). Lenses were immobilized in a glass bottom 6-well plate on the equatorial region using 1% agarose.

Analysis of mitochondrial integrity in secondary fibre cells was assessed using the Zeiss CLSM 510 META system connected to an Axiovert 200 inverted microscope. All micrographs were taken using the water immersion C-Apochromat (colour corrected) 40x objective (NA 1.2). Rhodamine 123 fluorescence was visualized using an argon/krypton laser with a 514 nm excitation laser line and a 560 nm long-pass emission filter. Micrographs of secondary fibre cells were taken for 0 μM (control), 50 μM, 200 μM, and 600 μM menadione treated lenses at 4, 24, and 48 hours post treatment.

Mitochondria were counted and their average and total lengths measured in micrographs of secondary fibre cells of the superficial cortex for each treatment group (0 μM, 50 μM, 200 μM, and 600 μM) at each time point (4, 24, and 48 hours post treatment) using analysis software designed at the University of Waterloo using the MATLAB programming language. Three micrographs from at least two different areas per lens were used in the analysis with three lenses per treatment group per time point for a total of 108 micrographs analyzed. For each micrograph, analysis consisted of retracing each individual mitochondrion using

both an automated process and the manual use of the fine adjustment tools of the analysis software to ensure that mitochondria information was correctly calculated.

3.5. Statistical analysis

3.5.1. Optical Function (Scantox Analysis)

Statistical analysis was undertaken using a two-way repeated measures analysis of variance (ANOVA) with Tukey or Bonfferoni post hoc tests. Results were considered significant at $p \leq 0.05$.

3.5.2. Mitochondrial Integrity

Mitochondrial count, average length, and total length were inspected using a two-way ANOVA with Tukey post hoc test. Results were considered significant at $p \leq 0.05$.

4. Results

4.1. Optical Function

Results of optical function assessment using the Scantox system to measure BVD variability following treatment by varying concentrations of menadione can be seen in Figure 2. No changes in BVD variability were observed within the 0 μM (control) and 50 μM treated lenses over time. While 200 μM treated lenses showed a trend of increasing BVD variability, this increase was not significant. Lenses treated with 600 μM menadione did show a significant increase in BVD variability over time at 24 hours ($p=0.0044$), 144 hours ($p<0.0000$), and 216 hours ($p<0.0000$) post treatment with respect to its pre-treatment (0 hours) time point. An increase in BVD variability over time was also seen for the 1000 μM treated lenses at 144 hours ($p<0.0000$) and 216 hours ($p=0.0002$) post treatment. Significant increases in BVD variability were also found between both the 600 μM and 1000 μM treated lenses versus the control group. For the 600 μM group, this increase was seen at 144 hours ($p<0.0000$) and 216 hours ($p=0.0007$) post treatment while it was only seen at 144 hours ($p<0.0000$) post treatment for the 1000 μM group.

While BVD variability in the 50 μM treated lenses was also smaller than that for the 600 μM (144 hours $p<0.0000$ and 216 hours $p<0.0000$) and the 1000 μM (144 hours $p=0.0002$) treated lenses, significant decreases in BVD variability were also seen from the 1000 μM treated lenses 216 hours ($p=0.0319$) post

Figure 2: Line graphs showing effects of 0 μM (control; black), 50 μM (blue), 200 μM (red), 200-A μM (purple), 200-B μM (pink), 600 μM (orange) and 1000 μM (green) menadione treatment on BVD variability (± standard error). Asterisks (*) denote significant changes ($p \leq 0.05$) in BVD variability with respect to its pre-treated scan (time 0). Daggers (†) denote significant changes in BVD variability with respect to the control group at the given time point. See text for more comparisons.

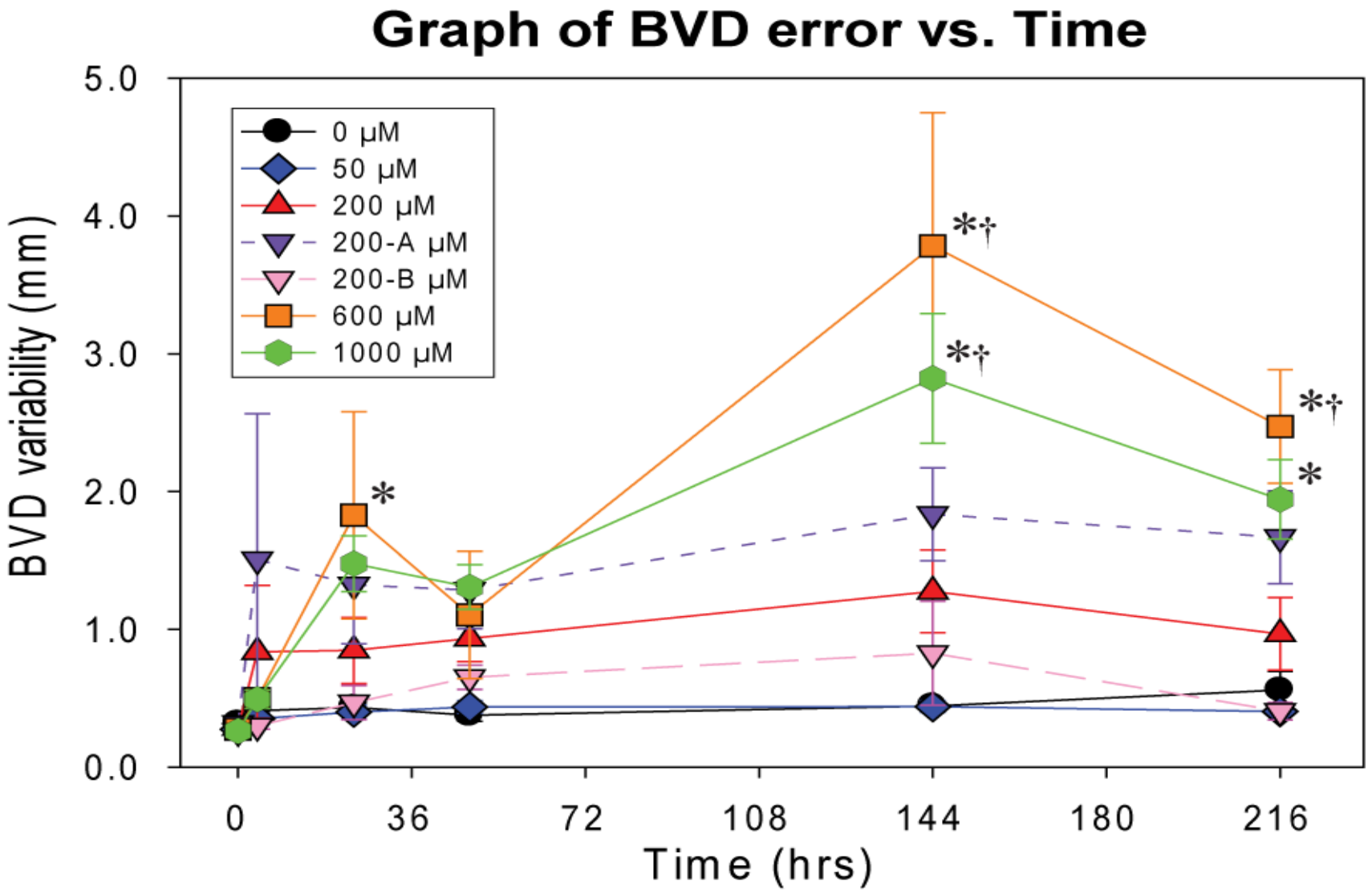
Graph of BVD error vs. Time
BVD variability (mm)
5.0
4.0
3.0
2.0
1.0
0.0
0 µM
50 µM
200 µM
200-A µM
200-B µM
600 µM
1000 µM
*
*†
*†
*†
*
0
36
72
108
144
180
216
Time (hrs)

treatment that was not observed in the control group. This would suggest the possibility that lenses treated with 50 μM menadione were better able to maintain their optic functionality, thereby sustaining a lower BVD variability, than those lenses not treated with any menadione.

Additionally, the 200 μM treated lenses had a lower BVD variability from the 600 μM treated lenses at 144 hours ($p<0.0000$) and 216 hours (0.0302) post treatment, while no differences were seen when compared to the 1000 μM group. It was assumed that the lack of significance with the 1000 μM group was due to the large range of BVD variability for the individual lenses within the 200 μM treatment group including the 216 hours post treatment results with a range from 0.263 mm to 2.466 mm. A deeper look into the 200 μM treatment group revealed that the lenses appeared to show two patterns of BVD variability. One pattern observed resembled the pattern seen for both the 0 μM and 50 μM treated lenses while the other resembled more closely that seen for the 600 μM and 1000 μM treated lenses.

Based on this observation, the 200 μM treated lenses were divided into two groups to see if there were two distinct patterns within this treatment group. To ensure no observation bias, 200 μM treated lenses were subdivided into 2 groups based on final BVD variability values. Those that fell within the ranges exhibited by 600 μM and 1000 μM treated lenses (BVD variability > 0.0964 mm) were categorized as 200-A ($n = 4$) while those outside of this range were categorized as

200-B (n = 5). The average BVD variability for 200-A was 1.668 ± 0.337 standard error while that of 200-B was 0.406 ± 0.064 standard error. Plots for the 200-A and 200-B groups were then added to the original graph as shown in Figure 2.

Statistical analysis was again carried out on these data using the 200-A and 200-B groups instead of the combined 200 μM group used before. No significant difference was detected overall between the 200-A treatment group with that of 600 μM and 1000 μM treated lenses, while the 200-B did show a significantly lower BVD variability compared to both 600 μM ($p=0.0055$) and 1000 μM ($p=0.0488$). These results would suggest that 200-B lenses follow the pattern seen for the 0 μM and 50 μM treated lenses while the 200-A lenses are similar to the 600 μM and 1000 μM treated lenses.

A correlation was observed in Figure 2 between an increase in BVD variability and an increase in size of the error bars (standard error of the BVD variability) indicating that the BVD variability was not consistent. It was also noted that occasionally one or more of the laser passages were unable to be recorded by the system's cameras. This is most likely due to the scattering of the light by the lens due to cataract formation (lens opacity) such that the cameras were unable to detect the path. The percentage of successful laser passages, along with the success range, is shown in Table 1. The data shows an inverse correlation to that seen for BVD variability and standard error increase; or in other words, as BVD

Table 1: Table showing the average percentage and range of beams that were successfully recorded by the Scantox system to be used in BVD variability analysis. Note the decrease in average percentage as a result of both time and concentration increase.

Time Post Treatment (hours)	% Beams						
	0 μM	50 μM	200 μM	200-A μM	200-B μM	600 μM	1000 μM
0	100 (100-100)	100 (100-100)	100 (100-100)	100 (100-100)	100 (100-100)	100 (100-100)	100 (100-100)
4	96.8 (68-100)	99 (91-100)	94.9 (64-100)	88.6 (64-100)	100 (100-100)	99.4 (95-100)	99 (95-100)
24	97.7 (86-100)	98.5 (91-100)	94.9 (86-100)	94.3 (86-100)	95.5 (91-100)	93.2 (59-100)	91.4 (73-100)
48	97.3 (91-100)	98 (91-100)	93.9 (68-100)	89.8 (68-100)	97.3 (95-100)	97.7 (95-100)	97 (91-100)
144	98.2 (91-100)	98 (95-100)	81.3 (55-100)	68.2 (55-100)	91.8 (55-100)	68.8 (23-100)	60.6 (45-77)
216	95.9 (86-100)	98.5 (95-100)	82.3 (55-100)	73.9 (55-100)	89.1 (68-100)	83 (36-100)	69.2 (45-100)

variability increased and the error bars became larger, the number of successful laser passages decreased (see 600 μM, 1000 μM and 200-A μM treated lenses at 114, and 216 hours post treatment time in Figure 2 and Table 1).

4.2. Secondary Fibre Cell Mitochondrial Integrity

Results for the average length of mitochondria, the number of mitochondria (count), and the combined mitochondrial length of confocal microscopic micrographs are shown in Table 2. Statistical analysis showed a difference between the 50 μM and 600 μM groups overall ($p=0.0087$) for average length, with those of the 50 μM treated lenses being longer.

Analysis of the number of mitochondria per micrograph showed significantly higher number of mitochondria in the 200 μM treated lenses than is seen for the 0 μM treated lenses ($p=0.0217$) and 50 μM ($p=0.0306$) treated lenses 48 hours post treatment. A significant increase in the number of mitochondria was also within the 200 μM treated lenses over time from 4 hours to 48 hours ($p=0.0027$) and as well as from 24 hours to 48 hours ($p=0.0096$). Although significant difference was not seen for the total mitochondrial length, the 200 μM treated lenses showed a trend toward an increasing total mitochondrial length over time, while that of the 600 μM treated tended to decrease. There was also a sharp rise in the total mitochondrial length for 50 μM treated lenses 24 hours post treatment, concurrent

Table 2: Table showing the average length of mitochondria, the number of mitochondria (count), and total length of mitochondria for confocal microscopy micrographs analysed using a Matlab image analysis program. Asterisk (*) denotes significant change ($p \leq 0.05$) with respect to its 4 hour time point. Dagger (†) denotes significant change with repect to 0 μM treated lenses at the given time point.

Time (hours)	Treatment	Average Length (μm)	Count	Total Length (μm)
4	0 μM	7.6 ± 1.3	244 ± 10	1848 ± 275
	50 μM	8.7 ± 2.2	248 ± 27	2205 ± 799
	200 μM	7.9 ± 0.8	165 ± 57	1286 ± 416
	600 μM	5.9 ± 1.0	380 ± 36	2232 ± 469
24	0 μM	7.1 ± 1.7	329 ± 29	2322 ± 464
	50 μM	8.2 ± 2.7	379 ± 105	3229 ± 1610
	200 μM	6.4 ± 2.6	214 ± 73	1414 ± 767
	600 μM	5.1 ± 2.6	431 ± 286	1730 ± 781
48	0 μM	7.7 ± 3.3	247 ± 57	1814 ± 788
	50 μM	8.2 ± 2.9	260 ± 33	2051 ± 636
	200 μM	3.7 ± 0.9	607 ± 190*†	2114 ± 635
	600 μM	3.6 ± 0.6	447 ± 52	1618 ± 451

with a rise in mitochondrial count, while average length remained constant, though these finding were not statistically significant.

Qualitative assessment of the mitochondria of the secondary fiber cells show a general trend for smaller mitochondria to appear with an increase in both menadione treatment concentration and time. Representative confocal micrographs showing the mitochondria of the treatment groups and time points are shown in Figure 3. These data suggest that since with an increase in menadione concentration and time following treatment, there is a decrease in average length, increase in number of mitochondria, with only a slight increase (for 200 μM treated lenses) or decrease (for 600 μM treated lenses) in total length of mitochondria, it is expected that a shift in the distribution of mitocondria toward an increase in relative frequency of shorter mitochondria will occur.

Frequency distribution histograms were generated for each analyzed micrograph to look at the overall distribution of the mitochondria, to see what percentage of each length of mitochondria was present in the micrograph. A shift in the distribution to the left would indicate an increase in smaller mitochondria, disappearance of larger ones, or a combination of the two. As the longest observed mitocondria was 112.29 μm in length, histogram plots with 57 bins of 2 μm increments were used. For presentation purposes histogram plots showing only the first 13 bins, comprising of at least 95% of the total number of mitochondria, are shown in Figure 4. The bin labels indicate the bin centre (i.e.

Figure 3: Representative confocal micrographs of mitochondria in secondary fibre cells for 0 μM (A), 50 μM (B), 200 μM (C), and 600 μM (D) treated lenses at 4 (1), 24 (2), and 48 (3) hours. Scale bar represents 20 μM. Note the increase in number of smaller mitochondria as concentration and time increase.

0 μM
50 μM
200 μM
600 μM
4 hours
24 hours
48 hours
A.1
B.1
C.1
D.1
A.2
B.2
C.2
D.2
A.3
B.3
C.3
C.3
20 μm

Figure 4: Histogram plots showing the relative distribution of mitochondrial length for 0 μM (A), 50 μM (B), 200 μM (C), and 600 μM (D) for 4 hours (1), 24 hours (2) and 48 hours (3), post treatment. Only the first 13 bins, comprising a minimum of 95% of the total mitochondrial count, are shown. For comparative purposes, percentages are shown on each graph indicating the cumulative relative frequency of mitochondria up to bin 11 (i.e. percentage mitochondria ≤ 12 μm long). Asterisks (*) denote significant change over time within a given concentration treatment group with respect to the 4 hour time point. Daggers (†) denote a significant change in relative distribution for a given bin size with repect to 0 μM treated lense. Note the general shift toward the left, indicating a greater relative frequency for smaller mitochondria, as a function of both time and concentration.

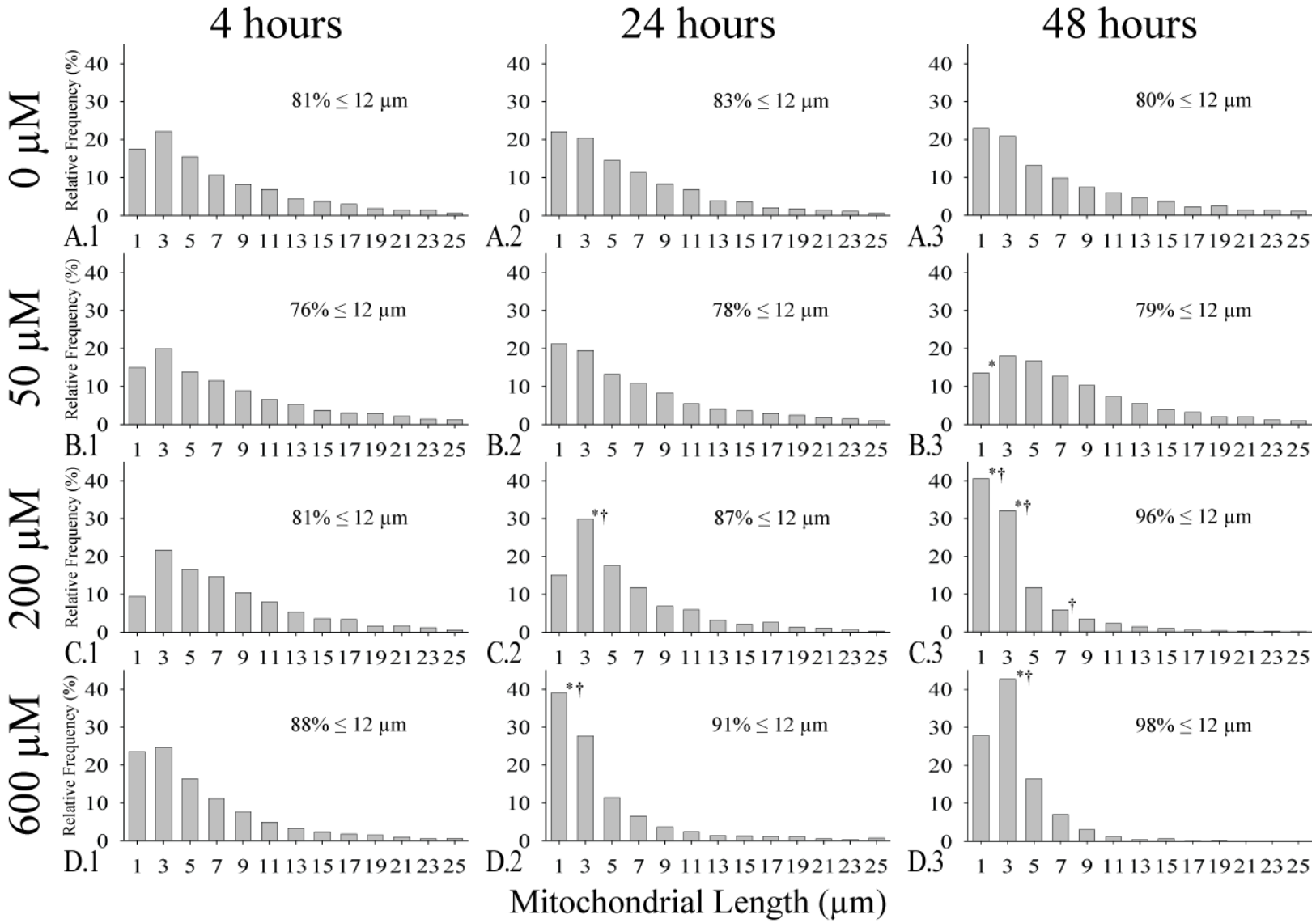
4 hours
24 hours
48 hours
0 µM
50 µM
200 µM
600 µM
Relative Frequency (%)
81% ≤ 12 µm
83% ≤ 12 µm
80% ≤ 12 µm
76% ≤ 12 µm
78% ≤ 12 µm
79% ≤ 12 µm
81% ≤ 12 µm
87% ≤ 12 µm
96% ≤ 12 µm
88% ≤ 12 µm
91% ≤ 12 µm
98% ≤ 12 µm
A.1
A.2
A.3
B.1
B.2
B.3
C.1
C.2
C.3
D.1
D.2
D.3
Mitochondrial Length (µm)

bin 1 is for mitochondria between 0 and 2 μm long). Herein, the bin centre will be used to identify the bin of interest. The cumulative relative frequency is shown on each histogram for bin 11 for comparison purposes.

Analysis of relative frequency distribution histograms indicated a shift in a mitochondrial length distribution in both a time and concentration dependent manner. As expected, no change in distribution was detected for the 0 μM or 50 μM treatment groups over time. The 200 μM treated lenses showed a shift toward a higher relative frequency of shorter mitochondria for both the 24 hour (bin 3; $p=0.0504$) and 48 hour (bins 1, 3, and 7; $p=0.0002$, $p=0.0002$, and $p=0.0115$ respectively) time points when compared with the 4 hour time point. A similar shift was observed for the 600 μM treated lenses at the 24 hour (bin 1; $p=0.0002$) and 48 hour (bin 3; $p=0.0002$) time points compared to the 4 hour time point. These results show a time dependent relative increase in shorter mitochondria as seen in the 200 μM and 600 μM treated lenses.

A concentration dependent effect was seen with a relative increase in shorter mitochondria for both the 200 μM (bin 3; $p=0.0012$) and 600 μM (bin 3; $p=0.0002$) treated lenses compared to the 0 μM treatment group at the 24 hour time point. The same increase in shorter mitochondria was found at the 48 hour time point for 200 μM (bins 1 and 3; $p=0.0002$ and $p=0.0003$) and 600 μM (bin 3; $p=0.0002$) treated lens compared to the 0 μM treatment group. Along with these findings, the significant decrease in bin 7 ($p=0.0115$) between 0 μM and 200 μM

treated lenses show that lenses treated with an increasing amount of menadione (> 50 μM) have a higher relative distribution of shorter mitochondria. In contrast, the 50 μM treated lenses showed a decrease in relative distribution for the shorter mitochondria (bin 1; $p=0.0015$) at the 48 hour time point compared with the 0 μM treatment group indicating a shift toward a higher relative distribution of longer mitochondria.

5. Discussion

5.1. Optical Function following Menadione Treatment

Treatment of menadione on bovine lenses has both a concentration and time dependent effect on the optical functionality of the lens, measured by the degree with which light can be focused onto a single point. Figure 2 shows that as the concentration of the menadione increases, BVD variability also increases overall as can be seen from 50 μM to 200 μM and from 200 μM to 600 μM treatment. This same trend, however does not appear to hold true when going from 600 μM to 1000 μM. This is likely due to a maximum concentration being reached at which point cells have become saturated with menadione and, as a result, increasing the concentration past that point would have no additional effect. An increase in BVD variability was also shown to be time dependent as can be seen, and statistically shown, for both the 600 μM and 1000 μM treatment groups. This same trend was seen with the 200-A μM treatment group, however, this was not shown statistically, most likely due to its low power.

It has been demonstrated that lens optical properties can recover from treatment by toxic substances (Bantseev et al., 2003a). Though not statistically significant, the same was found to be true for the 200-B group between the 144 and 216 hour time points (Figure 2). It would appear as though at least partial recovery is also seen elsewhere. From the 24 to 48 hour time points of the 600 μM group, a sharp decline in the BVD variability is seen before it again rises

(Figure 2). This is likely due to the lens partially overcoming the toxic effects of menadione before being overwhelmed by the toxin. This trend of partial recovery is also seen in the 1000 μM group between 24 and 48 hours, and the 200-A μM group between 4 and 24 hours; both of which are followed by a rise again in BVD variability. There also appears to be a second partial recovery from the 144 to 216 hour time points for the 600 μM and 1000 μM groups.

There are two possibilities as to why this is observed. The first, and less likely reason could be due to a cyclic effect of damage, followed by recovery repeated over and over until the cell eventually recovers completely or dies, though there has been no experimental proof suggesting that such a system exists. It is more likely that this effect seen at the 216 hour post treatment scan is pseudo-recovery due to the limitations of the experiment.

From Table 1, a correlation is seen between the percentage of successfully recorded laser beams and the BVD variability. It appears that as BVD variability increases, fewer beams are recorded. As the lens become more damaged, fewer beams pass through the range of the Scantox system's ability to record since they are scattered in such a way that the cameras on the system cannot collect the data. Therefore, it is likely that the laser passages that would result in the greatest BVD variability increase are excluded by the system. In this case, the more damaged a lens became, after a certain point, the better the BVD variability may actually appear, since the "worst" data is excluded from the analysis. This discrepancy,

however, would only exist when attempting to determine between a "really damaged" lens and a "really, really damaged" lens.

Earlier studies have shown that small concentrations of menadione can actually be beneficial to mitochondria with defects in the electron transport chain as they can act as electron carriers (Shneyvays et al., 2005). Though not statistically significant, these data show a trend for the 50 μM concentration group to have a lower BVD variability on average than the control with smaller variance among lenses (smaller standard error). This is easily seen at the 216 hour time point where the 1000 μM group was shown to statistically be significantly different than the 50 μM group, but not the control ($p=0.0317$, Figure 2). This observation coincides with the previous findings and indicates that menadione may in fact play a positive role in healthy mitochondria in low concentrations.

These findings appear to be examples of the effect known as hormesis, the common observation that low levels of toxicological treatments actually results in a positive effect (Calabrese and Baldwin, 2002). Though the mechanism behind this effect is unknown and its existence even disputed, some believe that repair mechanisms activated due to the low levels of toxins also repair other damage sustained that would have otherwise gone undetected (Rattan, 2008).

The most surprising finding was that lenses treated with 200 μM menadione could easily be sub-divided into one of two groups, based on whether BVD variability increase was sustained, or whether it recovered. As 200-B μM group

was found to be significantly different from 600 μM and 1000 μM treated groups while the 200-A μM group is not suggests that there is something unique to this concentration. Likely, this concentration is near some concentration limit from which bovine lenses can recover such that some do, and some do not.

5.2. Menadione effects on Mitochondrial Integrity

5.2.1. Average Length, Count and Total Length

Despite the lack of statistically significant findings for average length, mitochondrial count, and total length, most likely a result of low power (the micrograph analysis is highly labour intenstive and analysis of 108 micrographs is equivalent to only n = 3), many trends begin to emerge when looking at the data (Table 2). One significant finding that was found when looking at the mitochondrial average length, was that mitochondria in the 50 μM treated lenses had a much higher average length than those of the 600 μM treated lenses overall. Even though this difference was not significant for the 0 μM treated lenses ($p=0.0654$), it is very likely that this is only due to the low power of the analysis. The 200 μM treated lenses show similar average lengths to that of 0 μM and 50 μM treated lenses at the 4 hours post treatment, but this similarity quickly disappears and by 48 hours, the average length resembles that of the 600 μM treated lenses. This suggests that there is a time component to the effect of menadione on mitochondria corresponding to our results of the Scantox system.

The average length of the mitochondria in the 600 μM treated lenses is initially lower than that for the other three treatment groups and continues to decrease over time. This initially lower average length is likely due to a faster effect on the mitochondria than was seen for the 200 μM treatment group due to its higher concentration, suggesting a concentration dependent component to the effects of menadione, similar to the results of the Scantox system. The decrease in average length is accompanied by both an increase in the number of mitochondria and a decrease in the combined mitochondrial length, suggesting that the effects of menadione are causing the mitochondria to break apart into smaller fragments.

The mechanism underlying the mitochondrial fragmentation is speculated to be free-radical induced solidification, or hardening, of the normally fluid and free flowing lipoprotein membrane followed by the shattering of the membrane resulting in fragmentation. This mechanism was previously shown to exist in mitochondria in the presence of hydoxyl radicals (Dean et al., 1986). If this were to occur in the mitochondria seen in this study, it is likely that areas of the mitochondria affected greatest by menadione break apart and in some cases re-form into smaller mitochondria serving, in part, to eliminate those sections of the mitochondria that are damaged.

The average number of mitochondria per micrograph appears to be consistent over time for the 0 μM treated lenses and only a slight increase at 24 hours post treatment for the 50 μM treated lenses. There are a couple of

possibilities for this increase in the number of mitochondria. The first is simply due to low sample size. A second possibility corresponds to previously mentioned findings that low levels of menadione are in fact beneficial to mitochondria, as seen in the Scantox results. If this were the case, not only an increase in the number of mitochondria would be expected, as this could occur simply by mitochondria being broken apart into smaller pieces, but also an increase in overall "amount" of mitochondria. Indeed at 24 hours this is what is observed. The average length of mitochondria has not fallen, indicating that mitochondria are not simply being broken up, and an increase in the combined length of mitochondria is seen with the highest recorded value of 3229 ± 1610 μm (Table 2).

5.2.2. Frequency Distribution

Frequency distribution histograms were generated to look at the overall distribution of the mitochondrial lengths. Distribution of each treatment group over time is first be examined, followed by a look at the distributions for the varying treatment groups within a time point. Though not statistically significant, the histogram showing a shift to the right for the 50 μM treated lenses at 48 hours (Figure 4, Table 2) supports the idea that the increase in mitochondria number and total mitochondrial length, while the average mitochondrial length did not decrease, was not due to an increase in the number of shorter ones, but of longer mitochondria.

Distribution plots for the 600 μM show a definite trend in a shift to the left with 98.5% of mitochondria found by bin 11 as compared to only 80.0% of mitochondria being found by bin 11 for the 0 μM treatment group at the same time. This is supportive of the theory that mitochondria are being broken up into smaller fragments as a result of the menadione treatment. These results suggest that there is indeed a time dependent effect of menadione on the distribution of mitochondrial length.

Within the 4 hour post treatment histogram plots, no significant changes are seen indicating that the distribution of mitochondrial lengths was generally the same for all concentration groups (Figure 4). Within the 24 hours post treatment histograms, a large increase in the percentage of mitochondria of bin 3 with an accompanying decrease in bin 1 is seen for the 200 μM treated lenses. One possibility for this observation is that small mitochondria cannot resist the effects of mitochondria as well as larger ones, and therefore those that were small at the time of treatment were quickly destroyed and disappeared, leaving behind the larger ones that could withstand the negative effects longer. This is not likely the case as in fact no decrease in the percentage of small mitochondria when compared with its 4 hour results is seen, but is likely due to the breaking up of larger mitochondria into smaller ones. The 600 μM treated lenses show a shift to the left with a significant increase in mitochondria of bin centre 1, likely due to a great number of larger mitochondria breaking down into smaller fragments. These

findings suggest that indeed there is a concentration dependent effect of menadione on the distribution of mitochondrial length.

Within the 48 hour post treatment results the same slight shift to the right in the 50 μM treatment group, as was observed earlier, is seen. Both the 200 μM and 600 μM treated lenses show a significant increase in distribution of the smaller mitochondria. From this is can be seen that menadione has both a time and concentration dependent effect on mitochondrial distribution, resulting in an increase in smaller mitochondria.

In summary, results from the Scantox system showed a time dependent and concentration dependent effect on the BVD variability of the lens indicating a loss in optical function with increased menadione concentration treatment and time (Figure 2). Concurrently, confocal microscopy micrograph analysis of mitochondria of the secondary fibre cells showed a time dependent and concentration dependent effect on the mitochondria (Figure 3; Figure 4; Table 2). These results suggest a direct correlation between mitochondria integrity and morphology with the optic functionality of the lens. The mitochondrial changes also appear to precede those of BVD variability indicating that increase in BVD variability is the result of the changes in mitochondria and not the other way around. Results of the 50 μM menadione treated lenses strengthen the idea that mitochondria and optical function are directly linked as an increase in the mitochondria total length and a shift in distribution toward longer mitochondria in

the confocal micrographs is seen while a slightly lower BVD variability than control vehicle lenses is observed. Further work into the effects of mitochondrial breakdown and cytoskeletal integrity would confirm the role of the cytoskeleton in optic function and cataract formation which has been suggested for years (Tagliavini et al., 1986).

References

Amos, L.A., and A. Klug, 1974. Arrangement of Subunits in Flagellar Microtubules. Journal of Cell Science 14: 523-549.

Ashkin, A., K. Schutze, J.M. Dziedzic, U. Euteneuer, and M. Schliwa, 1990. Force Generation of Organelle Transport Measured Invivo by an Infrared-Laser Trap. Nature 348: 346-348.

Augusteyn, R.C., C.E. Jones, and J.M. Pope, 2008. Age-related development of a refractive index plateau in the human lens: evidence for a distinct nucleus. Clin Exp Optom 91: 296-301.

Azuma, M., E. Inoue, T. Oka, and T.R. Shearer, 1995. Proteolysis by Calpain Is an Underlying Mechanism for Formation of Sugar Cataract in Rat Lens. Current Eye Research 14: 27-34.

Azuma, M., T. Nakajima, E. Nakajima, and T.R. Shearer, 2003. Selenite may cause mitochondrial damage and cell death in cultured lens epithelial cells. Investigative Ophthalmology & Visual Science 44: U322-U322.

Babcock, G.T., and M. Wikstrom, 1992. Oxygen Activation and the Conservation of Energy in Cell Respiration. Nature 356: 301-309.

Baines, C.P., R.A. Kaiser, N.H. Purcell, N.S. Blair, H. Osinska, M.A. Hambleton, E.W. Brunskill, M.R. Sayen, R.A. Gottlieb, G.W. Dorn, J. Robbins, and J.D. Molkentin, 2005. Loss of cyclophilin D reveals a critical role for mitochondrial permeability transition in cell death. Nature 434: 658-62.

Bantseev, V., and J.G. Sivak, 2005. Confocal laser scanning microscopy imaging of dynamic TMRE movement in the mitochondria of epithelial and superficial cortical fiber cells of bovine lenses. Mol Vis 11: 518-23.

Bantseev, V., A.P. Cullen, J.R. Trevithick, and J.G. Sivak, 2003a. Optical function and mitochondrial metabolic properties in damage and recovery of bovine lens after in vitro carbonyl cyanide m-chlorophenylhydrazone treatment. Mitochondrion 3: 1-11.

Bantseev, V., D. McCanna, A. Banh, W.W. Wong, K.L. Moran, D.G. Dixon, J.R. Trevithick, and J.G. Sivak, 2003b. Mechanisms of ocular toxicity using the in vitro bovine lens and sodium dodecyl sulfate as a chemical model. Toxicol Sci 73: 98-107.

Bantseev, V.L., K.L. Herbert, J.R. Trevithick, and J.G. Sivak, 1999. Mitochondria of rat lenses: distribution near and at the sutures. Curr Eye Res 19: 506-16.

Bassnett, S., 1995. The fate of the Golgi apparatus and the endoplasmic reticulum during lens fiber cell differentiation. Invest Ophthalmol Vis Sci 36: 1793-803.

Bassnett, S., 1997. Fiber cell denucleation in the primate lens. Invest Ophthalmol Vis Sci 38: 1678-87.

Bassnett, S., 2002. Lens organelle degradation. Exp Eye Res 74: 1-6.

Bassnett, S., and G. Duncan, 1988. The influence of pH on membrane conductance and intercellular resistance in the rat lens. J Physiol 398: 507-21.

Bassnett, S., and D.C. Beebe, 1992. Coincident loss of mitochondria and nuclei during lens fiber cell differentiation. Dev Dyn 194: 85-93.

Bassnett, S., and D. Mataic, 1997. Chromatin degradation in differentiating fiber cells of the eye lens. J Cell Biol 137: 37-49.

Beauvoit, B., T. Kitai, and B. Chance, 1994. Contribution of the mitochondrial compartment to the optical properties of the rat liver: a theoretical and practical approach. Biophys J 67: 2501-10.

Benedek, G.B., 1971. Theory of Transparency of Eye. Applied Optics 10: 459-&.

Benedetti, E.L., I. Dunia, C.J. Bentzel, A.J.M. Vermorken, M. Kibbelaar, and H. Bloemendal, 1976. Portrait of Plasma-Membrane Specializations in Eye Lens Epithelium and Fibers. Biochimica Et Biophysica Acta 457: 353-384.

Bhatnagar, A., N.H. Ansari, L.F. Wang, P. Khanna, C.S. Wang, and S.K. Srivastava, 1995. Calcium-Mediated Disintegrative Globulization of Isolated Ocular Lens Fibers Mimics Cataractogenesis. Experimental Eye Research 61: 303-310.

Bornfeld, N., W. Breipohl, and G.J. Bijvank, 1974. Scanning Electron-Microscopy of Zonule of Zinn .1. Human Eyes. Albrecht Von Graefes Archiv Fur Klinische Und Experimentelle Ophthalmologie 192: 117-129.

Brunsting, A., and P.F. Mullaney, 1974. Differential light scattering from spherical mammalian cells. Biophys J 14: 439-53.

Burns, R.G., 1991. Alpha-Tubulin, Beta-Tubulin, and Gamma-Tubulins - Sequence Comparisons and Structural Constraints. Cell Motility and the Cytoskeleton 20: 181-189.

Calabrese, E.J., and L.A. Baldwin, 2002. Defining hormesis. Hum Exp Toxicol 21: 91-7.

Candia, O.A., and A.C. Zamudio, 2002. Regional distribution of the Na+ and K+ currents around the crystalline lens of rabbit. American Journal of Physiology-Cell Physiology 282: C252-C262.

Chow, C.T., and J.B. Biale, 1957. Metabolic Processes in Cytoplasmic Particles of the Avocado Fruit .2. Participation of Cytochrome-C in the Electron Transport Chain. Physiologia Plantarum 10: 64-75.

Criddle, D.N., S. Gillies, H.K. Baumgartner-Wilson, M. Jaffar, E.C. Chinje, S. Passmore, M. Chvanov, S. Barrow, O.V. Gerasimenko, A.V. Tepikin, R. Sutton, and O.H. Petersen, 2006. Menadione-induced reactive oxygen species generation via redox cycling promotes apoptosis of murine pancreatic acinar cells. J Biol Chem 281: 40485-92.

Dahm, R., C. Gribbon, R.A. Quinlan, and A.R. Prescott, 1998. Changes in the nucleolar and coiled body compartments precede lamina and chromatin reorganization during fibre cell denucleation in the bovine lens. Eur J Cell Biol 75: 237-46.

de Heredia, M.L., and R.P. Jansen, 2004. mRNA localization and the cytoskeleton. Current Opinion in Cell Biology 16: 80-85.

De Marchi, U., P. Pietrangeli, L. Marcocci, B. Mondovi, and A. Toninello, 2003. L-Deprenyl as an inhibitor of menadione-induced permeability transition in liver mitochondria. Biochem Pharmacol 66: 1749-54.

Dean, R.T., S.M. Thomas, and A. Garner, 1986. Free-radical-mediated fragmentation of monoamine oxidase in the mitochondrial membrane. Roles for lipid radicals. Biochem J 240: 489-94.

Desai, A., and T.J. Mitchison, 1997. Microtubule polymerization dynamics. Annual Review of Cell and Developmental Biology 13: 83-117.

Dische, Z., E. Borenfreund, and G. Zelmenis, 1956. Proteins and Protein Synthesis in Rat Lenses with Galactose Cataract. Archives of Ophthalmology 55: 633-642.

Dische, Z., J. Elliott, E. Pearson, and G.R. Merriam, 1959. Changes in Proteins and Protein Synthesis - in Tryptophane Deficiency and Radiation Cataracts of Rats. American Journal of Ophthalmology 47: 368-379.

Eckert, R., P. Donaldson, J.S. Lin, J. Bond, C. Green, R. Merriman-Smith, M. Tunstall, and J. Kistler, 2000. Gating of gap junction channels and hemichannels in the lens: A role in cataract? Gap Junctions 49: 343-356.

Fleischer, S., H. Klouwen, and G. Brierley, 1961. Studies of Electron Transfer System .38. Lipid Composition of Purified Enzyme Preparations Derived from Beef Heart Mitochondria. Journal of Biological Chemistry 236: 2936-&.

Frey, T.G., and C.A. Mannella, 2000. The internal structure of mitochondria. Trends Biochem Sci 25: 319-24.

Fukui, H.N., H. Obazawa, and J.H. Kinoshita, 1976. Lens Growth in Nakano Mouse. Investigative Ophthalmology 15: 422-425.

Gennis, R.B., 1998. Protein structure - Cytochrome c oxidase: One enzyme, two mechanisms? Science 280: 1712-1713.

Gibbons, I.R., 1981. Cilia and Flagella of Eukaryotes. Journal of Cell Biology 91: S107-S124.

Gray, M.W., G. Burger, and B.F. Lang, 1999. Mitochondrial evolution. Science 283: 1476-1481.

Gross, S.P., 2004. Hither and yon: a review of bi-directional microtubule-based transport. Physical Biology 1: R1-R11.

Habermann, A., T.A. Schroer, G. Griffiths, and J.K. Burkhardt, 2001. Immunolocalization of cytoplasmic dynein and dynactin subunits in cultured macrophages: enrichment on early endocytic organelles. Journal of Cell Science 114: 229-240.

Harding, C.V., J.R. Reddan, N.J. Unakar, and M. Bagchi, 1971. The control of cell division in the ocular lens. Int Rev Cytol: 215-300.

Hatefi, Y., 1985. The Mitochondrial Electron-Transport and Oxidative-Phosphorylation System. Annual Review of Biochemistry 54: 1015-1069.

Hatefi, Y., and K.E. Stempel, 1969. Isolation and Enzymatic Properties of Mitochondrial Reduced Diphosphopyridine Nucleotide Dehydrogenase. Journal of Biological Chemistry 244: 2350-&.

Hatefi, Y., and Y.M. Galante, 1980. Isolation of Cytochrome-B560 from Complex Ii (Succinate-Ubiquinone Oxidoreductase) and Its Reconstitution with Succinate-Dehydrogenase. Journal of Biological Chemistry 255: 5530-5537.

Haworth, R.A., and D.R. Hunter, 1979. The Ca2+-induced membrane transition in mitochondria. II. Nature of the Ca2+ trigger site. Arch Biochem Biophys 195: 460-7.

Helfand, B.T., P. Loomis, M. Yoon, and R.D. Goldman, 2003. Rapid transport of neural intermediate filament protein. Journal of Cell Science 116: 2345-2359.

Hunter, D.R., R.A. Haworth, and J.H. Southard, 1976. Relationship between configuration, function, and permeability in calcium-treated mitochondria. J Biol Chem 251: 5069-77.

Inoue, S., and E.D. Salmon, 1995. Force Generation by Microtubule Assembly Disassembly in Mitosis and Related Movements. Molecular Biology of the Cell 6: 1619-1640.

Itoh, H., A. Takahashi, K. Adachi, H. Noji, R. Yasuda, M. Yoshida, and K. Kinosita, 2004. Mechanically driven ATP synthesis by F-1-ATPase. Nature 427: 465-468.

Iyanagi, T., and I. Yamazaki, 1970. One-Electron-Transfer Reactions in Biochemical Systems .5. Difference in Mechanism of Quinone Reduction by Nadh Dehydrogenase and Nad(P)H Dehydrogenase (Dt-Diaphorase). Biochimica Et Biophysica Acta 216: 282-&.

Kasthurirangan, S., E.L. Markwell, D.A. Atchison, and J.M. Pope, 2008. In vivo study of changes in refractive index distribution in the human crystalline lens with age and accommodation. Invest Ophthalmol Vis Sci 49: 2531-40.

Kirschner, M., and T. Mitchison, 1986. Beyond Self-Assembly - from Microtubules to Morphogenesis. Cell 45: 329-342.

Kuszak, J., J. Alcala, and H. Maisel, 1980. The Surface-Morphology of Embryonic and Adult Chick Lens-Fiber Cells. American Journal of Anatomy 159: 395-410.

Kuszak, J.R., M.S. Macsai, K.J. Bloom, J.L. Rae, and R.S. Weinstein, 1985. Cell-to-Cell Fusion of Lens Fiber Cells Insitu - Correlative Light, Scanning Electron-Microscopic, and Freeze-Fracture Studies. Journal of Ultrastructure Research 93: 144-160.

Laux, I., and A. Nel, 2001. Evidence that oxidative stress-induced apoptosis by menadione involves Fas-dependent and Fas-independent pathways. Clin Immunol 101: 335-44.

Leung, K.H., and P.C. Hinkle, 1975. Reconstitution of Ion-Transport and Respiratory Control in Vesicles Formed from Reduced Coenzyme Q Cytochrome-C Reductase and Phospholipids. Journal of Biological Chemistry 250: 8467-8471.

Mannella, C.A., 2000. Introduction: Our changing views of mitochondria. Journal of Bioenergetics and Biomembranes 32: 1-4.

Margolis, R.L., and L. Wilson, 1998. Microtubule treadmilling: what goes around comes around. Bioessays 20: 830-836.

Mathias, R.T., 1985. Epithelial Water Transport in a Balanced Gradient System. Biophysical Journal 47: 823-836.

Mathias, R.T., and J.L. Rae, 1985. Transport-Properties of the Lens. American Journal of Physiology 249: C181-C190.

Mathias, R.T., J.L. Rae, and R.S. Eisenberg, 1981. The lens as a nonuniform spherical syncytium. Biophys J 34: 61-83.

Mathias, R.T., J.L. Rae, and G.J. Baldo, 1997. Physiological properties of the normal lens. Physiological Reviews 77: 21-50.

Mcavoy, J.W., 1978. Cell-Division, Cell Elongation and Distribution of Alpha-Crystallins, Beta-Crystallins and Gamma-Crystallins in Rat Lens. Journal of Embryology and Experimental Morphology 44: 149-165.

McCarty, C.A., and H.R. Taylor, 1996. Recent developments in vision research: Light damage in cataract. Investigative Ophthalmology & Visual Science 37: 1720-1723.

McDonald, D., M.A. Vodicka, G. Lucero, T.M. Svitkina, G.G. Borisy, M. Emerman, and T.J. Hope, 2002. Visualization of the intracellular behavior of HIV in living cells. Journal of Cell Biology 159: 441-452.

Melki, R., M.F. Carlier, D. Pantaloni, and S.N. Timasheff, 1989. Cold Depolymerization of Microtubules to Double Rings - Geometric Stabilization of Assemblies. Biochemistry 28: 9143-9152.

Morris, R.L., and P.J. Hollenbeck, 1993. The Regulation of Bidirectional Mitochondrial Transport Is Coordinated with Axonal Outgrowth. Journal of Cell Science 104: 917-927.

Nakagawa, T., S. Shimizu, T. Watanabe, O. Yamaguchi, K. Otsu, H. Yamagata, H. Inohara, T. Kubo, and Y. Tsujimoto, 2005. Cyclophilin D-dependent mitochondrial permeability transition regulates some necrotic but not apoptotic cell death. Nature 434: 652-8.

Nishimoto, S., K. Kawane, R. Watanabe-Fukunaga, H. Fukuyama, Y. Ohsawa, Y. Uchiyama, N. Hashida, N. Ohguro, Y. Tano, T. Morimoto, Y. Fukuda, and S. Nagata, 2003. Nuclear cataract caused by a lack of DNA degradation in the mouse eye lens. Nature 424: 1071-4.

Noji, H., and M. Yoshida, 2001. The rotary machine in the cell, ATP synthase. Journal of Biological Chemistry 276: 1665-1668.

Noji, H., R. Yasuda, M. Yoshida, and K. Kinosita, 1997. Direct observation of the rotation of F-1-ATPase. Nature 386: 299-302.

O'Rahilly, R., and D.B. Meyer, 1959. The early development of the eye in the chick. Gallus Domesticus (stages 8 to 25). Acta Anatomica: 20-58.

Ozaki, Y., A. Mizuno, K. Itoh, and K. Iriyama, 1987. Intermolecular and Intramolecular Disulfide Bond Formation and Related Structural-Changes in the Lens Proteins - a Raman-Spectroscopic Study Invivo of Lens Aging. Journal of Biological Chemistry 262: 15445-15551.

Palade, G.E., 1952. The Fine Structure of Mitochondria. Anatomical Record 114: 427-451.

Panda, D., H.P. Miller, and L. Wilson, 2002. Determination of the size and chemical nature of the stabilizing "cap" at microtubule ends using modulators of polymerization dynamics. Biochemistry 41: 1609-1617.

Paterson, C.A., 1972. Distribution and Movement of Ions in Ocular Lens. Documenta Ophthalmologica 31: 1-&.

Paterson, C.A., M.C. Neville, R.M. Jenkins, and Nordstro.Dk, 1974. Intracellular Potassium Activity in Frog Lens Determined Using Ion Specific Liquid Ion-Exchanger Filled Microelectrodes. Experimental Eye Research 19: 43-48.

Perkins, G.A., and T.G. Frey, 2000. Recent structural insight into mitochondria gained by microscopy. Micron 31: 97-111.

Rattan, S.I., 2008. Hormesis in aging. Ageing Res Rev 7: 63-78.

Robinson, K.R., and J.W. Patterson, 1983. Localization of Steady Currents in the Lens. Current Eye Research 2: 843-847.

Sanderson, J., J.M. Marcantonio, and G. Duncan, 1996. Calcium ionophore induced proteolysis and cataract: Inhibition by cell permeable calpain antagonists. Biochemical and Biophysical Research Communications 218: 893-901.

Seland, J.H., 1992. The Lens Capsule and Zonulae. Acta Ophthalmologica 70: 7-12.

Senior, A.E., and J. Weber, 2004. Happy motoring with ATP synthase. Nature Structural & Molecular Biology 11: 110-112.

Shearer, T.R., H. Ma, C. Fukiage, and M. Azuma, 1997. Selenite nuclear cataract: review of the model. Mol Vis 3: 8.

Shneyvays, V., D. Leshem, Y. Shmist, T. Zinman, and A. Shainberg, 2005. Effects of menadione and its derivative on cultured cardiomyocytes with mitochondrial disorders. J Mol Cell Cardiol 39: 149-58.

Smith, G.A., S.P. Gross, and L.W. Enquist, 2001. Herpesviruses use bidirectional fast-axonal transport to spread in sensory neurons. Proceedings of the National Academy of Sciences of the United States of America 98: 3466-3470.

Suomalainen, M., M.Y. Nakano, S. Keller, K. Boucke, R.P. Stidwill, and U.F. Geber, 1999. Microtubule-dependent plus- and minus end-directed motilities are competing processes for nuclear targeting of adenovirus. Journal of Cell Biology 144: 657-672.

Tagliavini, J., S.A. Gandolfi, and G. Maraini, 1986. Cytoskeleton abnormalities in human senile cataract. Curr Eye Res 5: 903-10.

Taylor, H.R., 1999. Epidemiology of age-related cataract. Eye 13 (Pt 3b): 445-8.

Thor, H., M.T. Smith, P. Hartzell, G. Bellomo, S.A. Jewell, and S. Orrenius, 1982. The Metabolism of Menadione (2-Methyl-1,4-Naphthoquinone) by Isolated

Hepatocytes - a Study of the Implications of Oxidative Stress in Intact-Cells. Journal of Biological Chemistry 257: 2419-2425.

Toninello, A., M. Salvi, M. Schweizer, and C. Richter, 2004. Menadione induces a low conductance state of the mitochondrial inner membrane sensitive to bongkrekic acid. Free Radic Biol Med 37: 1073-80.

Trayhurn, P., and R. Van Heyningen, 1972. The role of respiration in the energy metabolism of the bovine lens. Biochem J 129: 507-9.

Trokel, S., 1962. The Physical Basis for Transparency of the Crystalline Lens. Investigative Ophthalmology 1: 493-501.

Vale, R.D., T.S. Reese, and M.P. Sheetz, 1985a. Identification of a Novel Force-Generating Protein, Kinesin, Involved in Microtubule-Based Motility. Cell 42: 39-50.

Vale, R.D., B.J. Schnapp, T. Mitchison, E. Steuer, T.S. Reese, and M.P. Sheetz, 1985b. Different Axoplasmic Proteins Generate Movement in Opposite Directions Along Microtubules Invitro. Cell 43: 623-632.

Vanblerkom, J., 1991. Microtubule Mediation of Cytoplasmic and Nuclear Maturation during the Early Stages of Resumed Meiosis in Cultured Mouse Oocytes. Proceedings of the National Academy of Sciences of the United States of America 88: 5031-5035.

Vellai, T., and G. Vida, 1999. The origin of eukaryotes: the difference between prokaryotic and eukaryotic cells. Proceedings of the Royal Society of London Series B-Biological Sciences 266: 1571-1577.

Verrax, J., J. Stockis, A. Tison, H.S. Taper, and P.B. Calderon, 2006. Oxidative stress by ascorbate/menadione association kills K562 human chronic myelogenous leukaemia cells and inhibits its tumour growth in nude mice. Biochem Pharmacol 72: 671-80.

Wallin, I.E., 1923. The mitochondria problem. American Naturalist 57: 255-261.

Waterman-Storer, C.M., S.B. Karki, S.A. Kuznetsov, J.S. Tabb, D.G. Weiss, G.M. Langford, and E.L.F. Holzbaur, 1997. The interaction between cytoplasmic dynein and dynactin is required for fast axonal transport. Proceedings of the National Academy of Sciences of the United States of America 94: 12180-12185.

Weisenberg, R.C., and E.W. Taylor, 1968. Binding of Guanosine Nucleotide to Microtubule Subunit Protein Purified from Porcine Brain. Federation Proceedings 27: 299-&.

Wikstrom, M., K. Krab, and M. Saraste, 1981. Proton-Translocating Cytochrome Complexes. Annual Review of Biochemistry 50: 623-655.

Williams, D.L., 2006. Oxidation, antioxidants and cataract formation: a literature review. Veterinary Ophthalmology 9: 292-298.

Wilson, J.D., and T.H. Foster, 2007. Characterization of lysosomal contribution to whole-cell light scattering by organelle ablation. J Biomed Opt 12: 030503.

Wilson, J.D., W.J. Cottrell, and T.H. Foster, 2007. Index-of-refraction-dependent subcellular light scattering observed with organelle-specific dyes. J Biomed Opt 12: 014010.

Wu, X.F., and J.A. Hammer, 2000. Making sense of melanosome dynamics in mouse melanocytes. Pigment Cell Research 13: 241-247.

Zhang, D., and J.S. Armstrong, 2007. Bax and the mitochondrial permeability transition cooperate in the release of cytochrome c during endoplasmic reticulum-stress-induced apoptosis. Cell Death Differ 14: 703-15.

Zoratti, M., and I. Szabo, 1995. The mitochondrial permeability transition. Biochim Biophys Acta 1241: 139-76.